

INTERNATIONAL CONFERENCE  
ON  
MANUFACTURING AUTOMATION

N.W.M. KO

THE UNIVERSITY



OF HONG KONG

INTERNATIONAL  
CONFERENCE  
ON  
MANUFACTURING  
AUTOMATION

AUGUST 10, 11 and 12, 1992  
HONG KONG

PROCEEDINGS

*"Celebrating the 80th Anniversary of The University of Hong Kong"*

PROCEEDINGS

OF

THE INTERNATIONAL CONFERENCE

ON

MANUFACTURING AUTOMATION

August 10-12, 1992

HONG KONG

Organized

by

Department of Mechanical Engineering

The University of Hong Kong

Editors: N.W.M. Ko

S.T. Tan

**AUTOMATED PLANNING FOR ROBOTIC ASSEMBLY OF  
NON-CYLINDRICAL PARTS**

Y. L. Yao \*, W. Y. Cheng<sup>1</sup>, and S. Grewall<sup>2</sup>

<sup>\*</sup>School of Mechanical & Manufacturing Engineering,  
University of New South Wales, Australia  
<sup>1</sup>Department of Mechanical Engineering, University of Wollongong, Australia  
<sup>2</sup>Division of Manufacturing Technology, CSIRO, Australia

**ABSTRACT:** This paper describes development of an automated procedure by which a process planner with little knowledge about the robot dynamics can assess the maximum speed with which a given robot can accomplish its job without causing excessive contact forces/moments. Simulation studies were carried out first where the robot dynamic characteristics subject to contact forces/moments at its end effector were formulated and solved numerically. On the basis of that, a varying speed insertion motion was automatically synthesized. Experimental investigations involving mating of square pegs using a SCARA robot were carried out. The experimental results show that with such a varying speed motion, assembly operations can be carried out with a higher rate without causing large impact forces/moments at the initial contact. Therefore the automated planning system provides robotic assembly process planners with a user-friendly and effective means to achieve the optimum utilisation of industrial robots.

**1. INTRODUCTION**

Robots are not perfect in accomplishing certain assembly jobs. Variations due to dimensional tolerances of parts combined with misalignment due to the accuracy and repeatability may lead to jamming or even part damage. Misalignment between parts during automatic assembly can generate excessive contact forces/moments (Fig. 1) if the insertion speed is too high [12]. This may damage the parts and sometimes stall the assembly manipulator. To avoid this problem, comparatively lower insertion speed is commonly used in the insertion motion. This is based on the assumption that motions can take place in quasi-static manner. In order to achieve faster insertion, this assumption is not justified. Dynamic characteristics have to be taken into consideration. In past years, more work has been directed towards non-cylindrical part mating where angular misalignments become a significant problem.

Although, the uncertainty can be reduced by using some methods such as using tactile and vision sensors, the cost factor limits using expensive devices. Therefore, design engineers should be able to estimate whether an assembly task can be accomplished by a given robot without using special sensors or additional compliance devices. ElMaraghy [4] presented a method to examine the adequacy of selected dimensional tolerances and robot repeatability for automatic assembly of existing design.

Until recently, work has concentrated on the case of cylindrical peg-hole insertion. Examples of dynamic approach of part mating are presented by Asada[2] and Yao[12]. The strategy presented by Asada[2] uses a dynamic RCC hand for cylindrical part mating. It focuses on the inertial forces rather than the static spring forces. The requirement for the desired peg trajectory is to maintain the upright orientation while the peg slides along the chamfer. Yao [12] uses the passive mechanically compliant structure of the SCARA robots for the insertion of the cylindrical part mating. Because of the misplacements and misalignments, the peg always contacts the chamfer first. It can be relocated automatically in response to the contact forces established on the mating parts. Studying the case of non-cylindrical peg-hole insertion has been carried out under the quasi static assumption. Strategies have been proposed by Caine[3], Strip [9][10] and Wu [11]. Caine [3] presents a strategy for insertion of rectangular chamferless pegs. Different types of contact configurations are considered. From the quasi-static equilibrium, sets of forces and moments can be determined and can be applied onto the peg to move the peg to the correct position.

This paper presents a method for higher speed insertion of the non-cylindrical parts, without inducing excessive contact forces/moments. The varying-speed insertion method for cylindrical pegs presented by Yao [12] is extended to the non-cylindrical parts in this paper. Firstly, different cases of misalignments were considered and a geometric relationship between the insertion displacement along the z-axis and the lateral deflection and rotation in hand coordinate system [H] was derived. Then a dynamic simulation was carried out to predict the worst case in contact forces/moments and synthesise a varying speed insertion motion. Experimental application of the varying-speed motion showed improvement in terms of reduced operational cycle time and contact forces/moments.

**2. GEOMETRICAL MODEL FOR CHAMFER-CROSSING STAGE**  
Geometrical model is useful in determining the initial conditions for the simulation program, which will be discussed later. For simplicity, types of misalignments are considered only in case of positive translation and positive rotation (Fig. 2). The width of the contact chamfer surface area (L) can be shown as follows

$$L = b \sqrt{\frac{1 - 2 \tan \delta \theta_z}{(1 + \tan \delta \theta_z)} - 2 \max(\delta x, \delta y)} \quad (1)$$

To have a successful insertion, the misalignments of the peg as it contacts the hole must be small enough to ensure that the peg is guided into the hole. Therefore, the following equation should be satisfied:

$$B < b \sqrt{\frac{1 - 2 \tan \delta \theta_z}{(1 + \tan \delta \theta_z)} - 2 \max(\delta x, \delta y)} \quad (2)$$

where B is the width of the bottom of the chamfer. The height of the chamfer (h) is

$$h = \frac{b-B}{2} \tan \alpha \quad (3)$$

In determining how fast a square peg can be inserted, the insertion motion  $\Delta z(t)$  has to be determined according to the lateral and orientation response which eventually leads the peg into the hole. The faster the lateral response ( $\Delta x$  or  $\Delta y$ ) and the orientation response ( $\Delta \theta_z$ ), the faster insertion can be achieved. If the peg is inserted too fast, the chamfer will be pressed too hard and the contact force will momentarily increase to a fairly large value which may result in part damage. The relation of the insertion ( $\Delta z_r(t)$ ) due to translation is

$$\Delta z_r(t) = \Delta r(t) \tan \alpha \quad (4)$$

where  $\Delta r(t)$  is the greater value of  $\Delta x(t)$  and  $\Delta y(t)$ . Secondly, the relation of insertion ( $\Delta z_r(t)$ ) due to rotation ( $\Delta \theta_z(t)$ ) is considered. Let the width of the peg be b, the angle of the chamfer  $\alpha$ , the angular misalignment  $\delta \theta_z$ , and  $\Delta \theta_z$  the angular increment due to rotation, the depth of the chamfer inserted due to rotation is

$$z_r = \frac{b \tan \alpha (1 - \frac{1}{(\cos \delta \theta_z + \sin \delta \theta_z)})}{2} \quad (5)$$

taking differentiation of both sides of (5), one obtains

$$\Delta z_r = \frac{b \tan \alpha}{2} (1 - \frac{\sin \delta \theta_z - \cos \delta \theta_z}{(\cos \delta \theta_z + \sin \delta \theta_z)^2}) \Delta \theta_z \quad (6)$$

The total insertion  $\Delta z$  equals to the sum of insertion due to lateral deflection ( $\Delta z_r(t)$ ) and insertion due to rotation ( $\Delta z_r(t)$ ), i.e.

$$\Delta z = \max(\Delta x, \Delta y) \tan \alpha + \frac{b \tan \alpha}{2} (1 - \frac{\sin 8\theta_z - \cos 8\theta_z}{\cos 8\theta_z + \sin 8\theta_z}) \Delta \theta_z \quad (7)$$

### 3. SIMULATION

For a given robot, simulation can be carried out as follows. Firstly, the contact forces  $F_x(t)$ ,  $F_y(t)$  and the induced torque  $\tau_z(t)$  are specified in the hand coordinate system (H) and corresponding torques of joints are calculated by

$$\tau(t) = J_H^T(t) [F_x(t) \ F_y(t) \ \tau_z(t)]^T \quad (8)$$

where  $J_H(t)$  is the 3x3 Jacobian matrix written in (H). Then, the dynamic formulation can be solved numerically

$$\dot{\theta} = M^{-1}(\theta) \{ \tau - V(\theta, \dot{\theta}) + K(\theta, \theta_0) \} \quad (9)$$

Lastly, the results are converted back to (H) by

$$[\Delta x(t) \ \Delta y(t) \ \Delta \theta_z(t)] = J_H(t) \Delta \theta(t) \quad (10)$$

The input values of  $F_x(t)$ ,  $F_y(t)$  and  $\tau_z(t)$  were assumed to be step functions and various step sizes were investigated. Using the numerical method which is based on Runge-Kutta method and procedure outlined above, the responses of at the tool  $\Delta x(t)$ ,  $\Delta y(t)$  and  $\Delta \theta_z(t)$  as well as their derivatives were obtained as shown in Fig. 3.

### 4. EXPERIMENT RESULTS AND DISCUSSION

The goal of the experiment was firstly to validate the prediction by the simulation program. Then the varying speed insertion method was compared with the conventional constant speed insertion method in terms of contact forces and moments, as well as the cycle time.

An ADEPT ONE SCARA type robot was used. The experiment involving the making of chamfered square peg into a square hole was conducted. In order to measure the contact forces and moments during the chamfer-crossing stage, an integrated force and moment sensor was mounted at the wrist, between the end of the forearm and the tool. Insertions were programmed for both the varying speed motion and constant speed motion.

To validate the simulation results, the peg was deliberately programmed to deviate a bit to simulate different cases of misalignments. The constant insertion speed method was used and the insertion speed was kept constant (10%) in all conditions. The worst case was the translation only misalignment ( $\Delta x + \Delta y$ ). The results were similar to that predicted by the simulation.

The second part of the experiments was to compare the varying speed insertion method with constant speed method. One of the example was in the case of combined rotation and translation misalignment with  $-\delta x_x - \delta y_y + \delta \theta_z$ . The induced contact forces were positive in both x and y direction. The induced moment in z direction was also positive. In the constant speed insertion, the peg approached the hole at 70% of full speed and remained the same speed in chamfercrossing stage. In the varying speed insertion, the peg was inserted in 100% of full speed in the approach stage and stopped just before it touched the chamfer. Then insertion was restarted using a lower speed (20% of the full speed). The result indicated that contact forces in x, y direction and moments in three directions were very similar. However, the excessive contact force in z axis was much smaller in the varying speed case (Fig. 4). It can be explained that using a lower insertion speed in chamfercrossing stage led to a smaller impact on the surface of the chamfer and the hole.

Then the experiment was to compare the maximum speed of insertion in both methods under the same condition. Again the same example as above was used. For the constant speed method, the insertion speed was gradually reduced from 70% until a speed at which no excessive contact force occurred. It was found that the safe speed was 0.5% of the full one and it took about 22 seconds from

starting to the end of the motion. For the varying speed insertion, the varying speed was decre: from 20% until the same safe condition was reached. It took only about 1.2 second for the whole process. Comparing the varying-speed insertion motion and the conventional constant-speed motion, it was found that while achieving less excessive contact force, the varying-speed insertion motion demonstrated a significant increase in cycle rates.

In the dynamic equation discussed before, it was assumed that there was no moment induced in the direction of x and y direction. However, they existed in the experiment. Since all the equations were based on the hand coordinate system and all the forces and moments were assumed to apply through the hand coordinate origin. Actually, the contact points were not on the hand coordinate origin. There was a certain distance  $d(t)$  between the hand coordinate origin and the contact points. The contact forces acted somewhere on the surface of the chamfer or the peg. Under such circumstances, three dimensional forces and moment about the z direction measured by the force sensor were as same as the values in the hand coordinate system. But the moments in x and y direction were not the same. They were equal to the following:

$$\begin{aligned} \tau_x(t) &= \tau_x(t) + d(t) F_y \\ \tau_y(t) &= \tau_y(t) + d(t) F_x \end{aligned} \quad (11)$$

where {F} refer to the coordinate in contact point.

### 5. CONCLUSION

The investigation into the assembly operation of the SCARA type robot has revealed that using the internal compliance of the robot is often practical and effective aid even for the non-cylindrical part mating. The varying speed insertion motion provides lower contact force/moments while increase cycle time.

### 6. REFERENCE

1. Arui, T., Makino, H., "Analysis of Part Insertion with Complicated Shapes," *Annals of the CIRP* 38: January 1989, pp. 17-20.
2. Asada, H., Kakumoto Y., "The Dynamic RCC Hand For High-Speed Assembly," *Proc. IEEE Intl. Conf. on Robotics and Automation*, PA., 1988, pp. 120-125.
3. Caine, M. E., Lozano-Perez, T., Seering, W. P., "Assembly Strategies for Chamferless Parts," *Proc. IEEE Intl. Conf. on Robotics and Automation*, PA., 1989, pp. 472-477.
4. ElMaraghy, H. A., ElMaraghy, W. H., Knoll, L., "Design Specification of Parts Dimensional Tolerance for Robotic Assembly," *Computers in Industry* 10: March 1988, pp. 47-59.
5. ElMaraghy, H. A., Johns, B., "An Investigation into the Compliance of SCARA Robots. Part I: Analytical Model," *ASME Trans. Journal of Dynamic Systems, Measurement and Control*, 110: 18-22, March 1988.
6. Gotschlich, S. N., Kak, A. C., "A Dynamic Approach to High-Precision Parts Mating," *Proc. IEEE Intl. Conf. on Robotics and Automation*, PA., 1988, pp. 1246-1253.
7. Nevins, J. L., Whitney, D. E., "Assembly Research," *Automatica* 16: 595-613, 1980.
8. Pat, D. K., Leu, M. C., "Feasible Tasks for Manipulators with Uncertainty and Compliance," *Proc of 1987 IEEE Intl. Conf. on Systems Man and Cybernetics*, PA., pp. 6-13.
9. Strip, D. R., "A Passive Mechanism for Insertion of Convex Pegs," *Proc. IEEE Intl. Conf. on Robotics and Automation*, PA., 1989, pp. 242-248.
10. Strip, D. R., "Insertion Using Geometric Analysis and Hybrid Force-position Control: Method and Analysis," *Proc. IEEE Intl. Conf. on Robotics and Automation*, PA., 1988, pp. 1744-1751.
11. Wu, M. H., Hopkins, S., "Strategy for Automatic Assembly of Spline Peg Hole Based on Stiffness Hybrid Control," *10th International Conference on Assembly Automation*, PA., 1989, pp. 95-105.
12. Yao, Y. L., "Transient Lateral Motion of Robots in Parting Mating," *Robotic & Computer Integrated Manufacturing*, Vol. 8, No. 2, 1991, pp. 103-111.

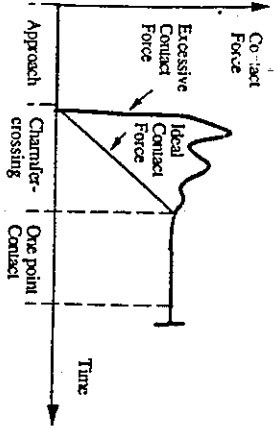


Fig. 1 Excessive and ideal contact force (moment)

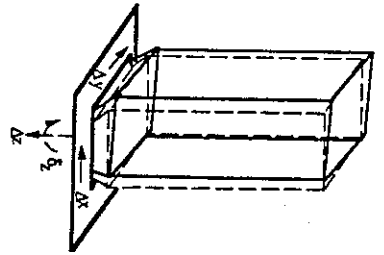


Fig. 2 Lateral response  $\Delta x$  and  $\Delta y$ , rotation response  $\Delta z$  and insertion motion  $\Delta z$

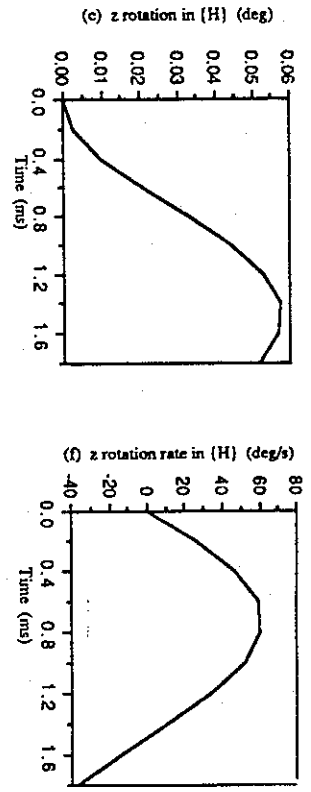
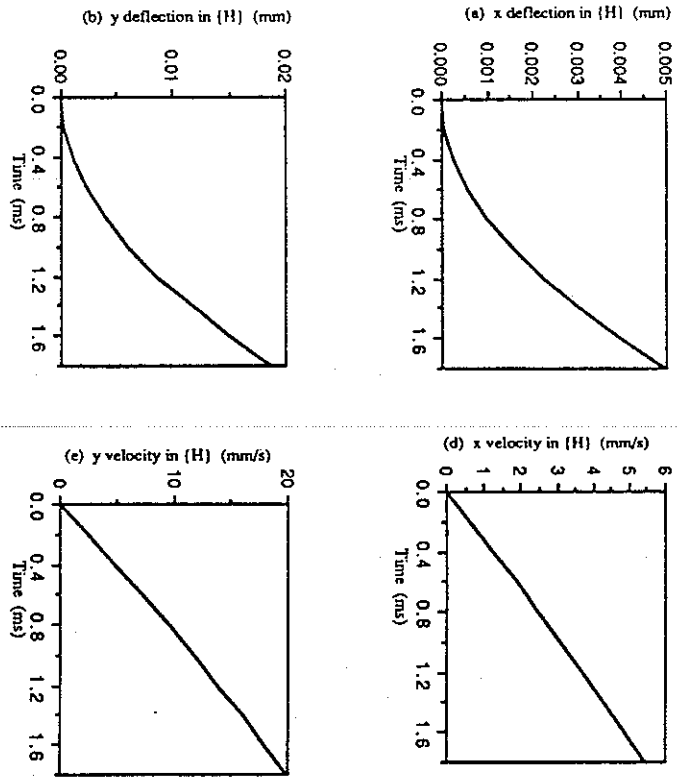


Fig. 3 Simulated end effector responses

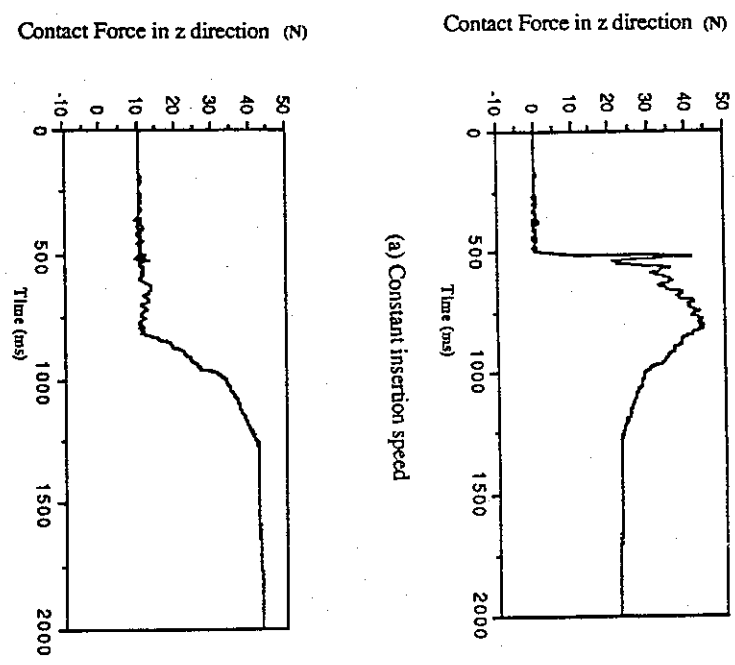


Fig. 4 Experimental Comparison